Simulation the Effects of High Sediment-laden Inundation Flow on the Variations of Floodplain in the Lower Yellow River Basin

Xinhua ZHANG[1], Hiroshi ISHIDAIRA[2], Kuniyoshi TAKEUCHI[3] and Satoru OISHI[4]

[1]Student member of JSCE, M. Eng., Graduated School of Engineering, University of Yamanashi (Takeda 4-3-11, Kofu, Yamanashi, Japan 400-8511)

[2]Member of JSCE, Dr. of Eng., Associate Prof., Interdisciplinary Graduate School of Medicine & Engineering University of Yamanashi, (Takeda 4-3-11, Kofu, Yamanashi, Japan 400-8511)

[3]Member of JSCE, Ph. D, Professor, Interdisciplinary Graduate School of Medicine & Engineering University of Yamanashi (Takeda 4-3-11, Kofu, Yamanashi, Japan 400-8511)

[4]Member of JSCE, Dr. of Eng., Associate Prof., Interdisciplinary Graduate School of Medicine & Engineering University of Yamanashi, (Takeda 4-3-11, Kofu, Yamanashi, Japan 400-8511)

Flood inundation due to dike-break or overtopping is a serious problem to cause great damages and losses to human beings, and thus threats the sustainable development in the suffered regions. In addition, flooding flows usually company with sediment transportations and yields. The sediment not only can worsen the damages, but also can change the elevations of floodplains. Now, flood inundation can be simulated successfully by 2-D shallow water equations (SWEs). The 2-D SWEs can also be coupled to transport equations to simulate the sediment transportation. However, problems of mass conservation and numerical instability may arise if the numerical schemes of simulation models are not chosen with cares when the sediment transport and variations of floodplains are coupled with the inundation model. For the purpose of overcome these problems, the Koren upwind scheme of third order accuracy is employed to discretize the advection terms of the sediment transportation equations. A case study was conducted in a small area of the lower Yellow River in China. Results of the case study demonstrate that the Koren scheme is robust and accurate for the coupled 2D SWEs and sediment transportation equations so that a precise estimation of floodplain variations can be made.

Key Words: *Flood inundation, Shallow water equation, Sediment transport, Bed variation of floodplain, Koren upwind scheme*

1. INTRODUCTION

Flood disaster has been an obstacle to the regional developments. Because of its destructive feature many experts have considered it in the context of sustainability[1)]. Despite the structural flood protection measures like dams and levees, or super-dikes, are absolutely needed to safeguard existing developments, for example, reinforced dikes, or super-dike, play an important part in flood protection of urban areas in Japan[2), 3)], they have also added additional flood risks due to their potential failures. An effective flood protection system is generally a mix of structural and non-structural measures. The latter approaches better conform to the spirit of sustainable development[1)].

In river basins such as the Yellow River in China, sediment transport is another prominent problem in the flood inundation because it is not only worsened the damage and losses caused by flooding, but also change the geomorphology of floodplains.

Flood inundation flow can be treated as vertically well-mixed water bodies in which the horizontal length scale are much greater than the vertical inundation depths. Two dimensional shallow water equations (SWEs) are the suitable mathematical equations of flooding flows. Many physical phenomena, such as storm surges, tidal fluctuations, tsunami waves, etc., can be studied by these equations. It can also be coupled with sediment transport equations to deal with erosion and deposition of sediment in riverbeds or floodplains.

Because the SWEs are a system of coupled non-linear partial differential equations, the numerical solutions of the SWEs are challengeable in addition to the difficulties of mathematical natures. Most important is the variable designations

of water depths and velocity because spurious oscillations may take place and lead to the simulated results without observing the law of mass conservation if the numerical algorithms are not chosen with cares. For example, the use of non-staggered grids in the finite difference context can lead to spurious spatial oscillations[4]. Therefore, the 2D staggered leap-frog explicit scheme (2D SLES)[5], developed by Iwasa et al (1980), are used to discretize the 2D SWEs. Because this numerical algorithm is quite stable and accurate, the flood inundation can be simulated without much effort.

Although the sediment transport can be incorporated into the numerical scheme of 2D SLES easily, the mass conservation of sediment transportation can not be guaranteed satisfactorily. In order to overcome such problem, a Koren upwind scheme of third-order accuracy[6] is adopted so that a build-in mechanism of mass conservation and minimizing oscillations can be constructed within the integrated numerical algorithms.

In this study, the integrated numerical algorithms have a three-layer structure. The first layer accounts for the 2D inundation flow, expressed by the conventional 2D SWEs. The second level calculates sediment carrying capacities and actual transport rates of uniform sediment on the basis of information obtained in the first layer. In the third layer the quantities of deposition and erosion are simulated based on the information provided by the first and second layers.

The main objectives of this study are firstly to simulate flood inundation and sediment transport due to sediment-laden flooding flows, and then to evaluate the variations of floodplain due to the deposition and erosion in the inundation flows.

In this paper, 2D shallow water equations and the 2D non-equilibrium sediment transportation model are introduced in section 2. In section 3, numerical algorithms to the governing equations are explained, especially the Koren upwind scheme of third order accuracy for the mass conservation of sediment transportations. A case study was conducted in the Yellow River basin and the results are presented in section 4. Finally, a concluding remark is made in section 5.

2. GOVERNING EQUATIONS OF FLOOD INUNDATION AND SEDIMENTAL TRANSPORT

Under the assumptions of a hydrostatic pressure and a vertical uniform velocity profile, the widely used 2D SWEs can be obtained by vertical integration of the Navier-Stokes equations. The 2D SWEs for flood inundation are usually expressed in a Cartesian coordinate system in the following form:

$$\frac{\partial h}{\partial t}+\frac{\partial M}{\partial x}+\frac{\partial N}{\partial y}=0 \tag{1}$$

$$\frac{\partial M}{\partial t}+\frac{\partial (uM)}{\partial x}+\frac{\partial (vM)}{\partial y}=-gh\frac{\partial H}{\partial x}-\frac{\tau_{bx}}{\rho} \tag{2}$$

$$\frac{\partial N}{\partial t}+\frac{\partial (uN)}{\partial x}+\frac{\partial (vN)}{\partial y}=-gh\frac{\partial H}{\partial y}-\frac{\tau_{by}}{\rho} \tag{3}$$

where h is the inundated water depth; $M(=uh)$ and $N(vh)$ are discharge flux per unit width in x- and y-orientation, respectively; u and v are flow velocity in x and y directions; g is gravitational acceleration; H is surface water level which equals to Z_b+h, here, Z_b is the ground elevation. ρ is mass density of water flow; τ_{bx} , τ_{by} are ground shear stresses in x and y directions, respectively. They can be estimated by the equations as follows:

$$\tau_{bx}/\rho = gn^2u\sqrt{u^2+v^2}/h^{1/3} \tag{4}$$

$$\tau_{by}/\rho = gn^2v\sqrt{u^2+v^2}/h^{1/3} \tag{5}$$

where n is Manning roughness coefficient.

Because suspended sediment concentration is not equal to the carrying capacity of the inundation flow, the non-equilibrium 2D transport of sediment is used and given by

$$\frac{\partial (hS)}{\partial t}+\frac{\partial (huS)}{\partial x}+\frac{\partial (hvS)}{\partial y}= \varepsilon_s[\frac{\partial^2 (hS)}{\partial x^2}+\frac{\partial^2 (hS)}{\partial y^2}]+\alpha\omega(S_*-S) \tag{6}$$

where S means suspended sediment concentrations in the inundated flooding flow; S_* is sediment carrying capacity; ε_s is sediment diffusion coefficient; α is the parameter related to depositions or erosions; ω is settling velocity; and other variables are the same as those in the 2D SWEs. In this study, sediment diffusion coefficient ε_s is considered to be the same as eddy viscosity, which can be written in the depth-averaged form as

$$\varepsilon_s = \kappa u_* h/6 \tag{7}$$

where κ=Karman constant and u_*=bed shear velocity. The shear velocity u_* is described by the following equation:

$$u_* = \frac{\sqrt{g}}{C}\sqrt{u^2+v^2} \tag{8}$$

where C=Chezy coefficient.

The carrying capacity of uniform sediment can be expressed by[7), 8)]

$$S_* = K_c\left(\frac{(\sqrt{u^2+v^2})^3}{h\omega}\right)^m \tag{9}$$

where K_c and m =coefficients (K_c=0.02, m=0.92 for the case study). The units of S_* *(or K_c)*, u *(or v, or ω)*, and h are kg/m^3, m/s and m, respectively.

In the condition dominated by suspended sediment,

bed morphological change can be expressed as

$$\rho' \frac{\partial Z}{\partial t} = \alpha\omega(S - S_*) \tag{10}$$

where ρ'=dry density of bed material; Z= the bed elevation; and t=time. The bed elevation variation ΔZ resulting from sediment transport during a single time interval Δt can be calculated by the following formula:

$$\Delta Z = \frac{1}{\rho'}\alpha\omega(S - S_*)\Delta t \tag{11}$$

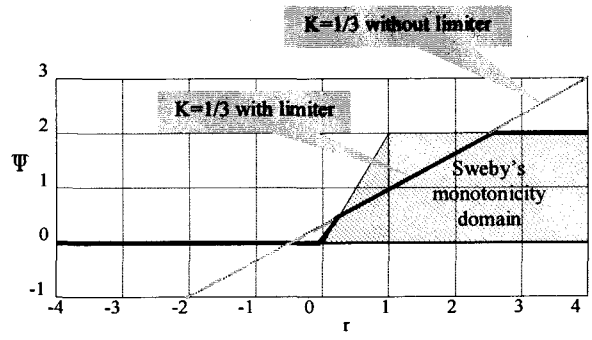

Fig. 1 Limiter $\Psi(r)$ and Sweby's monotonicity domain

3. NUMERICAL SCHEME

(1) Shallow water equations

For the facilitation of coupling 2D SWEs with the sediment transportation, a staggered leapfrog explicit 2D numerical algorithm, developed by Iwasa[5] et al in 1980 for the discretization of 2D SWEs, is used in this study for the flood inundation simulation. Please refer to the reference for details.

(2) Koren upwind scheme for the simulation of sediment transportation

In the flood inundation, sediments are transported together with the movement of flooding flow. Diffusive quantity due to the gradient differences of sediment concentrations is small compared with the advection quantity due to the movement of flooding flow. So, the advection dominates the diffusion in the sediment transport. The spatial discretization on the advection terms in Eq. (6) is crucial for the simulation of sediment transport because a spurious oscillation will occur if the scheme is not chosen with cares. For this purpose, the Koren upwind scheme of third accuracy is introduced to estimate the advection quantity because this scheme is accurate, stable and mass conservative.

To facilitate the explanation of Koren upwind scheme, the diffusion and non-equilibrium term on the right side of Eq. (6) are temporarily neglected.

Considering the following 2D advection equation

$$\frac{\partial S}{\partial t} + \frac{\partial F(S)}{\partial x} + \frac{\partial G(S)}{\partial y} = 0 \tag{12}$$

With flux function $F(S)=(uhS)$ in x-direction, and $G(S)=(vhS)$ in y-direction. In a uniform grid system, following discretization can be obtained

$$\frac{\partial S}{\partial t} + \frac{1}{h}\left(F_{i+1/2,j} - F_{i-1/2,j} + G_{i,j+1/2} - G_{i,j-1/2}\right) = 0 \tag{13}$$

Fluxes in x and y directions can be estimated analogously. Here, the flux in x- direction, for example, Koren interpolates it as follows:

$$F_{i+1/2,j} = F_{i,j} + \frac{1+\kappa}{4}(F_{i+1,j} - F_{i,j}) + \frac{1-\kappa}{4}(F_{i,j} - F_{i-1,j}) \tag{14}$$

$\kappa \in [-1,1]$

and similarly for $F_{i-1/2j}$.

Error analysis shows that the flux difference $(F_{i+1/2j}-F_{i-1/2j})$ is second order accurate, but becomes third-order accurate[6] when choosing $k=1/3$. Substituting k=1/3 into Eq. (13), the equation can be reformulated as follows:

$$\begin{aligned} F_{i+1/2,j} &= F_{i,j} + \frac{1}{3}(F_{i+1,j} - F_{i,j}) + \frac{1}{6}(F_{i,j} - F_{i-1,j}) \\ &= F_{i,j} + \frac{1}{2}\left[\frac{1}{3} + \frac{2}{3}r_{i+1/2,j}\right](F_{i,j} - F_{i-1,j}), \\ r_{i+1/2,j} &= \frac{F_{i+1,j} - F_{i,j}}{F_{i,j} - F_{i-1,j}} \end{aligned} \tag{15}$$

In order to avoid unwanted local maxima or minima (numerical oscillations), the Sweby monotonicity theory is followed, and thus Eq. (15) can been rewritten as

$$F_{i+1/2,j} = F_{i,j} + \frac{1}{2}\Psi(r_{i+1/2,j})(F_{i,j} - F_{i-1,j}) \tag{16}$$

where $\Psi(r_{i+1/2j})$ is the limiter function, which must be inside or at the boundary of Sweby's monotonicity domain. The limiter argument $r_{i+1/2j}$ is the upwind ratio of consecutive solution gradients. By introducing the limiter function

$$\Psi(r) = \max\left(0, \min\left(2r, \min\left(\frac{1}{3} + \frac{2}{3}r, 2\right)\right)\right) \tag{17}$$

into Eq. (16), monotonicity is obtained in the non-limited $k=1/3$ scheme. **Fig. 1** shows Sweby's monotonicity domain. The non-limited $k=1/3$ scheme is indicated by the dashed line. For $r<1/4$ *and* $r>5/2$ the scheme is out of the monotonicity domain. It can be directly seen that the limiter most consistent with the non-limited $k=1/3$ scheme, and that obeys the Sweby monotonicity rule is the one given by Eq. (16). The solid bold line in the figure corresponds to this limiter function.

For the same reason, Koren interpolates the flux in y- direction can be worked out

The interpolation cannot, however, be applied straightforwardly to and including the boundaries. In this study, interpolations are made by decreasing the accuracy to the first order in this condition. For the convenience of making computer program, the flux terms in Eq. (12) can be given in accordance with following conditions:

For the flux function $F=(uhS)$:

If $u_{i+1/2,j} \geq 0$:

$$
\begin{aligned}
&if \quad i=0: F_{1/2,j} = (u_{in})_j \left((hS)_{in}\right)_j, \\
&if \quad i=1: F_{3/2,j} = u_{3/2,j} \frac{1}{2}\left((hS)_{1,j} + (hS)_{2,j}\right), \\
&if \quad i=n: F_{n+1/2,j} = u_{n+1/2,j}\left((hS)_{n,j} + \frac{1}{2}\left((hS)_{n,j} - (hS)_{n-1,j}\right)\right), \\
&else \quad : F_{i+1/2,j} = u_{i+1/2,j}\left((hS)_{i,j} + \frac{1}{2}\Psi\left(r_{i+1/2,j}\right)\left((hS)_{i,j} - (hS)_{i-1,j}\right)\right) \\
&\qquad r_{i+1/2,j} = \frac{(hS)_{i+1,j} - (hS)_{i,j} + \varepsilon}{(hS)_{i,j} - (hS)_{i-1,j} + \varepsilon}
\end{aligned}
$$

Else:

$$
\begin{aligned}
&if \quad i=0: F_{1/2,j} = u_{1/2,j}\left((hS)_{1,j} + \frac{1}{2}\left((hS)_{1,j} - (hS)_{2,j}\right)\right), \\
&if \quad i=n-1: F_{n-1/2,j} = u_{n-1/2,j} \frac{1}{2}\left((hS)_{n,j} + (hS)_{n-1,j}\right), \\
&if, \quad i=n \quad : F_{n+1/2,j} = (u_{in})_j \left((hS)_{in}\right)_j \\
&else \quad : F_{i+1/2,j} = u_{i+1/2,j}\left((hS)_{i+1,j} + \frac{1}{2}\Psi\left(r_{i+1/2,j}\right)\left((hS)_{i+1,j} - (hS)_{i+2,j}\right)\right) \\
&\qquad r_{i+1/2,j} = \frac{(hS)_{i,j} - (hS)_{i+1,j} + \varepsilon}{(hS)_{i+1,j} - (hS)_{i+2,j} + \varepsilon}
\end{aligned}
$$

Endif,

And likewise, for the flux function $G=(vhS)$:

If $v_{i,j+1/2} \geq 0$:

$$
\begin{aligned}
&if \quad j=0: G_{i,1/2} = (v_{in})_i \left((hS)_{in}\right)_i, \\
&if \quad j=1: G_{i,3/2} = v_{i,3/2} \frac{1}{2}\left((hS)_{i,1} + (hS)_{i,2}\right), \\
&if \quad j=n: G_{i,n+1/2} = v_{i,n+1/2}\left((hS)_{i,n} + \frac{1}{2}\left((hS)_{i,n} - (hS)_{i,n-1}\right)\right), \\
&else \quad : G_{i,j+1/2} = v_{i,j+1/2}\left((hS)_{i,j} + \frac{1}{2}\Psi\left(r_{i,j+1/2}\right)\left((hS)_{i,j} - (hS)_{i,j-1}\right)\right) \\
&\qquad r_{i,j+1/2} = \frac{(hS)_{i,j+1} - (hS)_{i,j} + \varepsilon}{(hS)_{i,j} - (hS)_{i,j-1} + \varepsilon}
\end{aligned}
$$

Else:

$$
\begin{aligned}
&if \quad j=0: G_{i,1/2} = v_{i,1/2}\left((hS)_{i,1} + \frac{1}{2}\left((hS)_{i,1} - (hS)_{i,2}\right)\right), \\
&if \quad j=n-1: G_{i,n-1/2} = v_{i,n-1/2} \frac{1}{2}\left((hS)_{i,n} + (hS)_{i,n-1}\right), \\
&if, \quad j=n \quad : G_{i,n+1/2} = (v_{in})_i \left((hS)_{in}\right)_i, \\
&else \quad : G_{i,j+1/2} = v_{i,j+1/2}\left((hS)_{i,j+1/2} + \frac{1}{2}\Psi\left(r_{i,j+1/2}\right)\left((hS)_{i,j+1} - (hS)_{i,j+2}\right)\right) \\
&\qquad r_{i,j+1/2} = \frac{(hS)_{i,j} - (hS)_{i,j+1} + \varepsilon}{(hS)_{i,j+1} - (hS)_{i,j+2} + \varepsilon}
\end{aligned}
$$

Endif.

In the scheme, a small quantity of ε is introduced. In this study, $\varepsilon=1.0\times10^{-9}$ is used to guarantee no problems of division by zero in the simulation of sediment transportation.

A central-difference scheme of second-order accuracy is adopted to discretize the diffusion term on the right side of Eq. (6).

Bottom variations may be calculated after several time-steps of water simulation because its variations are very small in a small time-step.

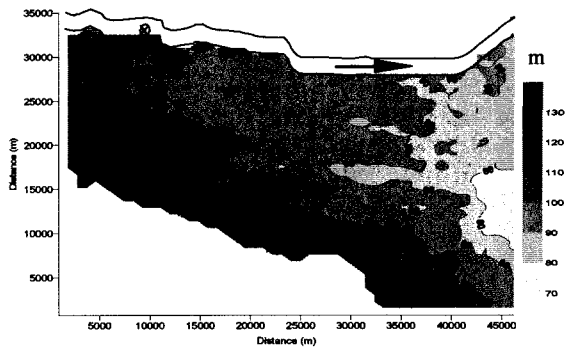

Fig. 2 Topography of study region (elevation map)

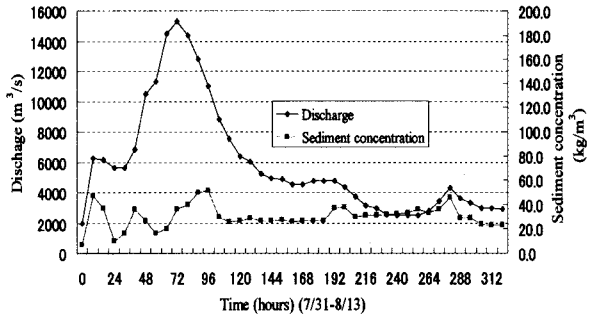

Fig.3 Flood discharge and sediment concentration in 1982 at Huayuankou station

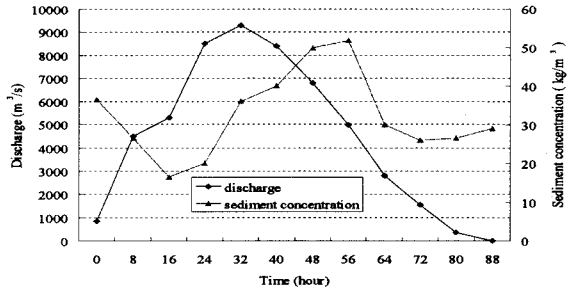

Fig.4 Assumed discharge and sediment concentration from Huayuankou break inlet in the flood of 1982

However, in this study, same time-step is used to maintain the accuracy and integrity of the system.

4. APPLICATION

(1) Study area

The Yellow River is famous in the world not only for its scale but also for the complicated problems due to the high concentrations of sediment. The average suspended concentration is about 30 kg/m^3 according to recent 50-year measured data. Flows with concentration over 200 kg/m^3 are frequently observed. The measured maximum concentration is more than 1000 kg/m^3. Sediment size is very fine; about 0.03 mm. Suspended sediments are dominant. So there is no need to consider the bed loads in the modeling[9].

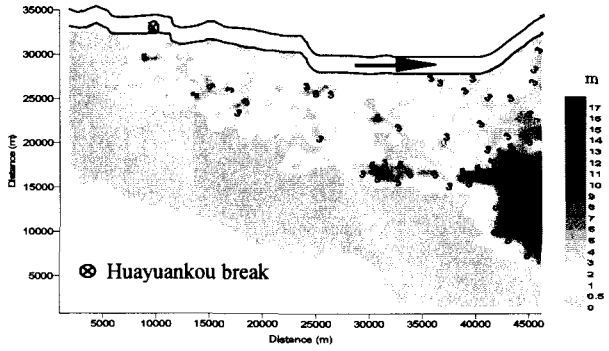

Fig.5 Inundated water depth distribution at the end of simulation (maximum water depth = 17.78 m)

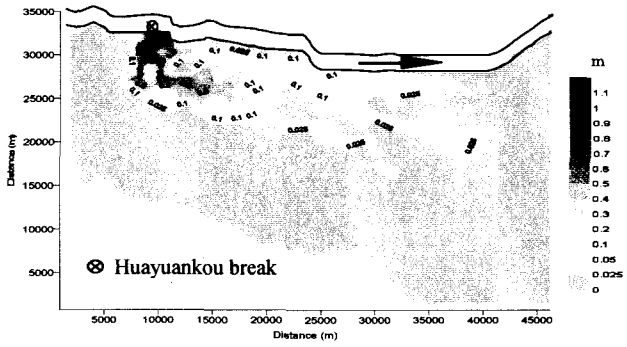

Fig.6 Deposition distribution at the end of simulation (maximum height = 1.17 m)

In this study, Huayuankou is assumed to be broken when a flood with a scale of 1982 flood occurred. For the purpose of testing model, an area of 50×50 km, subdivided by 1.0 km DEMs, is selected as the objective area of simulation. The x-direction is in the west-east wise, while the y-direction is in the south-north wise. The DEM of 1×1 km in this region has an accurate resolution of Δx=924.58 m and Δy=756.08 m. The ground elevation at the Huayuankou station is 101.00 m based on the DEM (**Fig. 2**).

(2) Boundary and initial conditions

Since the completion of Sanmenxia project in 1958, a flood event occurred from July 31 to August 13 of 1982 is the largest one observed. Its peak discharge reached 15,300 m^3/s and the sediment concentrations were in an averaged level. The observed discharges at Huayuankou station are shown in **Fig. 3**. It is supposed that the dike at the Huayuankou station is starting to break when the discharge in the river channel reaches 6,000 m^3/s. Based on this assumption, the inundation discharges are obtained, as shown in **Fig. 4**. It was used as the boundary condition. Other outer boundaries are supposed to be high walls as done by Iwasa[5] et al.

Before the breakage, the water depths in the floodplain are supposed to be zero, which is the initial condition.

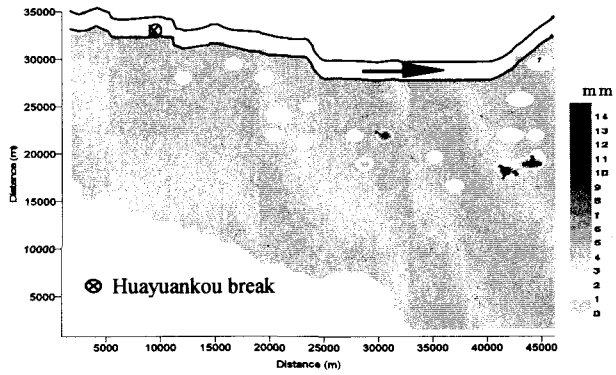

Fig.7 Erosion distribution at the end of simulation (maximum erosion = 14.88 mm)

Table 1 Statistics of simulated results

Area of Simulation	Meshes			1607
	Area (km^2)			1123.38
Inundated region	Clear water		Meshes	645
			Area (km^2)	450.89
			Volume based on water depth ($10^6 m^3$)	1524.24
			Volume from dike break ($10^6 m^3$)	1524.24
	Sediment	Quantity from break inlet (10^6 ton)		51.68
		Suspended	quantity 1(Koren) (10^6 ton)	0.12
			quantity 2 (10^6 ton)	0.49
		Deposition	Meshes	597
			Area (km^2)	417.34
			Quantity 1 (Koren)	51.63
			Quantity 2 (10^6 ton)	52.35
		Erosion	Meshes	48
			Area (km^2)	33.55
			Quantity 1(Koren)	0.07
			Quantity 2 (10^6 ton)	0.53

(3) Simulated results and discussions

The inundation in this stage of study is a hypothetical condition although the flood discharges and sediment concentrations are observed data. The simulated results have to be evaluated based on the mass conservations. The main objective of this study is to build up an integrated simulation model of inundation and sediment transportation. Therefore, the drainage measures in the study region are temporarily not included in this paper.

a) Spatial distribution of inundated water and water depths at the end of simulation

Based on the assumption of dike break, the simulation was continued for 88 hours. The total water volume from the break-inlet is 1524.24×10^6 m^3. When the simulation completed, the water volume based on the inundated water depths over the study region is completely equal to that volume, as displayed in **Table 1**. The distribution of water depths is shown in **Fig. 5**. Simulated water depths reflect quite well the topography by comparing **Fig. 5** with **Fig. 2**, the deepest value at the lowest mesh in the east reaches 17.78 m and the inundated area is 450.89 km^2, which accounts for 40.1% of the total area simulated. The inundated area will be further enlarged if the simulation is not restrained within 50 km downstream of Huayuankou station.

b) The variation of floodplain due to deposition and erosion of sediments

Generally, sediment transport in flows is typically in non-equilibrium conditions, which may result in deposition or erosion. In addition sediment granular sizes are not uniform. But for the special condition in the Yellow River basin, a uniformly granular size of 0.025 mm with an average settling velocity of 0.000299 m/s is used[9].

At the end of simulation, the variations of floodplain represented by the heights of deposition and erosion are shown in **Fig. 6** and **Fig.7**, respectively. It can be found in these figures that the deposition, which means the increase of floodplain, dominates the change of floodplain. For example, height of deposition that is greater than 2.5 cm reaches to an area of 417.34 km^2, accounting for 92.6% of the total inundated area. The nearer the locations to the break-inlet, the higher height of deposition is. The highest height is 117.0 cm at the vicinity of break-inlet. On the other hand, erosion seems not significant as displayed in **Fig.7**. Only 48 meshes have been eroded and the maximum height of erosion is 1.4 mm. The erosion are occurred almost when the inundation water are clear due to deposition.

The averaged sediment concentration of 1982 flood is 33.9 kg/m^3, which is almost equal to the muti-year average of 30.0 kg/m^3. If the total quantity of sediment in this flood is uniformly distributed on the inundated meshes, an averaged 11.5 cm increment of floodplain can be resulted. This value may also imply that the deposition is dominant factors of floodplain variation. Therefore, simulated results can provide very useful information on the variations of floodplain potentially affected by a dike-break at the Huayuankou station.

c) The effectiveness of Koren upwind scheme

Based on the Koren scheme, the total sediment quantity composed by the quantity from the break-inlet and the yield of erosion is 51.75×10^6 ton, while the quantity of suspension and deposition is also 51.75×10^6 ton. Please refer to **Table 1** for the details of these values. That is to say, the Koren upwind scheme can satisfactorily guarantee the mass conservation.

On the other hand, simulated results without adopting the Koren scheme indicate that the mass conservation is not strictly observed. For example the total quantity of deposition and suspension, 52.84×10^6 ton, is greater than the total available quantity, 52.21×10^6 ton, from the break inlet and the yield of erosion as shown in **Table 1** by the columns worded as "quantity 2". **Fig. 6** and **Fig. 7** are the results obtained by the Koren scheme.

5. CONCLUSIONS

In this study, an integrated simulation model of 2-D SWEs and 2-D non-equilibrium sediment transportation is developed for the simulation of floodplain variations in the lower Yellow River. In order to overcome the numerical instability, the Koren scheme of third-order accuracy is adopted. Compared with the simulated results without using this scheme, conclusions can be drawn like: 1) The integrated numerical algorithm of inundation and floodplain variations are accurate and reliable due to the high accuracy of Koren scheme; 2) The variation of floodplain due to the inundation flow with an averaged level of sediment concentrations is significantly large; 3) the floodplain variations are mainly dominated by sediment deposition and thus can lead to the increments of floodplain substantially; 4) the yields of sediment in the inundation process are not significant.

These results can also be explained by the formation of "suspended river" in the Lower Yellow River, in which the riverbed is 4-20 m higher than that behind the dikes. Therefore, the integrated model developed in this study has a potential to be applied to other floodplains, and it is possible to have different results of floodplain variations.

REFERENCES

1) Kundzewicz, Z. W. 2002. "Non-structural Flood Protection and Sustainability", IWRA, Water International, Vol. 27, No.1, pp.3-13.
2) Kundzewicz, Z. W. and Takeuchi, K. 1999, "Flood Protection and Management:Quo Vadimus?" Hydrological Science Journal, Vol.44, No.3, pp.417-432.
3) Takeuchi, K., 2002."Flood Management in Japan-From Rivers to Basins." IWRA, Water International, Vol. 27, No.1, pp.20-25.
4) Aizinger, V. and Dawson, C., 2002. "A discontinuous Galerkin method for two-dimensional flow and transport in shallow water," Adv Water Resour., Vol. 25, pp. 67-84.
5) Iwasa, Y, Inoue, K and Mizutori, M. (1980). Hydraulic analysis of overland flood flows by means of numerical method. Annuals of Disaster Prevention Research Institute, 23(B-2) 305-317. (in Japanese).
6) Holstad, A., 2001. "Temperature-driven fluid flow in porous media using a mixed finite element method and a finite volume method." Adv Water Res, Vol. 24, pp 843-862.
7) Guo, Q. C., 2002. "Modeling Nouniform Suspended Sediment Transport in Alluvial Rivers". J Hydr Eng, ASCE, Vol. 128(9), pp. 839-847.
8) Wuhan University of Hydraulic and Electric Engineering, 1990. "River Simulation", Water Resources and Electric Press (in Chinese).
9) Guo, Q. C., Takeuchi, K., Ishidaira, H. and Hu, C., 2002. "1-D Numerical Modeling of Sediment Transport in the Lower Yellow River." A Technical Report to the CREST of JST, pp. 1-26.

(Received September 30, 2003)